

This version of the manuscript is the final revised one of the published on-line on 29 March 2018:

<https://pubs.acs.org/doi/abs/10.1021/acs.jmedchem.8b00359>

Tetrahydroquinoline ring as a versatile bioisostere of tetralin for melatonin receptor ligands

Silvia Rivara,^a Laura Scalvini,^a Alessio Lodola,^a Marco Mor,^a Daniel-Henri Caignard,^b Philippe Delagrangé,^b Simona Collina,^c Valeria Lucini,^d Francesco Scaglione,^d Lucia Furiassi,^e Michele Mari,^e Simone Lucarini,^e Annalida Bedini,^e Gilberto Spadoni^{e*}

^a Dipartimento di Scienze degli Alimenti e del Farmaco, Università degli Studi di Parma, Parco Area delle Scienze 27/A I-43124 Parma, Italy.

^b Institut de Recherches Servier, 125 Chemin de Ronde, F-78290 Croissy sur Seine, France.

^c Dipartimento di Scienze del Farmaco, Università degli Studi di Pavia, Viale Taramelli 12, I-27100 Pavia, Italy.

^d Dipartimento di Oncologia ed Emato-oncologia, Università degli Studi di Milano, Via Vanvitelli 32, I-20129 Milano, Italy.

^e Dipartimento di Scienze Biomolecolari, Università degli Studi di Urbino “Carlo Bo”, Piazza Rinascimento 6, I-61029 Urbino, Italy.

Abstract

A new family of melatonin receptor ligands, characterized by a tetrahydroquinoline (THQ) scaffold carrying an amide chain in position 3, was devised as conformationally-constrained analogs of flexible *N*-anilinoethylamides previously developed. Molecular superposition models allowed to identify the patterns of substitution conferring high receptor binding affinity and support the THQ ring as a suitable scaffold for the preparation of melatonin ligands. The biological activity of 3-acylamino-THQs was compared with that of the corresponding tetralin derivatives. The THQ ring proved to be a versatile scaffold for easy feasible MT₁ and MT₂ ligands, which resulted as more polar bioisosteres of their tetralin analogs. Potent partial agonists, with sub-nanomolar binding affinity for the MT₂ receptor were obtained and a new series of THQ derivatives is presented. The putative binding mode of potent THQs and tetralines was discussed on the basis of their conformational equilibria as inferred from molecular dynamics simulations and experimental NMR data.

Introduction

Melatonin (*N*-acetyl-5-methoxytryptamine, **1**, Figure 1) is a tryptophan-derived hormone mainly secreted by the pineal gland following a circadian rhythm, with peak concentrations reached at night. In humans melatonin is also produced by other organs and tissues, such as the retina, gastrointestinal tract, lymphocytes, bone marrow and skin, leading to high local concentrations found in some body districts. This widespread distribution is correlated with the numerous physiological processes modulated by melatonin, which span from central nervous system (CNS)-related activities, such as the regulation of circadian rhythms, of the sleep-wake cycle and hormone secretion, to peripheral organs control. Peripherally, melatonin is involved in the modulation of the immune system, of retinal functions, in the homeostasis of glucose concentrations and of the cardiovascular system.¹

Alteration of melatonin secretion or transmission has been correlated with several pathological processes, like sleep disturbances and disrupted circadian rhythms, and a beneficial role of melatonin administration has been proposed for pathologies as diverse as neurodegenerative diseases, diabetes, multiple sclerosis and cancer.^{2,3}

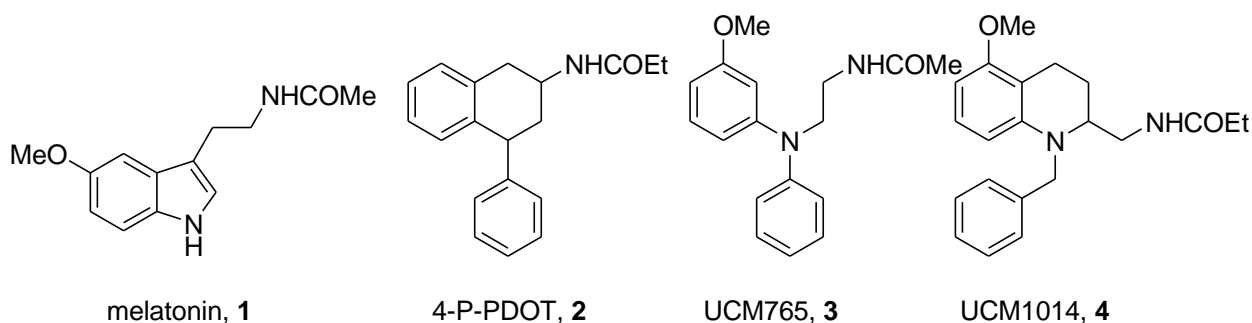


Figure 1. Structures of melatonin and melatonin receptor ligands.

Melatonin exerts many of its activities by activating two G protein-coupled receptors (GPCR), named MT₁ and MT₂. These receptors are mainly expressed in the CNS, particularly in the hypothalamic suprachiasmatic nucleus (SCN), but have also been detected in many peripheral tissues.⁴ In the last decades great efforts have been made in the biochemical and pharmacological characterization of these receptors. Melatonin signaling through GPCRs is not a mere redundant system, as could be assumed from MT₁ and MT₂ co-expression in many tissues and the similar affinity of melatonin for the two receptors. In fact, in different tissues, either one or the other receptor exerts a predominant activity, and in some cases the two receptors mediate opposite effects. The MT₁ receptor inhibits neuronal firing in mouse SCN, inhibits prolactin secretion in photoperiodic species, modulates visual function, affects lymphocyte differentiation and mediates vasoconstriction in rat caudal artery. The MT₂ receptor is mainly involved in phase-shifting of circadian rhythms in the SCN, promotion of non-REM sleep in mice and in rat caudal artery vasodilation.⁴ The complexity of melatonin receptors signaling and activity is further increased by their ability to couple with different G proteins, to homo-

and heterodimerize⁵ and to act as presynaptic heteroreceptors modulating the release of other neurotransmitters.^{4,6}

The understanding of the mechanisms underlying melatonin activity has led to the approval of synthetic receptor ligands for CNS-related pathologies. The nonselective MT₁/MT₂ agonists ramelteon and tasimelteon have obtained marketing authorization for insomnia and non-24-h sleep-wake disorder, respectively. Agomelatine, endowed with MT₁/MT₂ agonist and 5HT_{2c} antagonist activities, is prescribed for the treatment of major depression.⁷ Additionally, several receptor subtype-selective ligands have been prepared, with intrinsic activities spanning from full agonist, to partial agonist, antagonist and inverse agonist.⁸ These compounds include widely used pharmacological tools, such as the nonselective antagonist luzindole and the MT₂-selective partial agonist 4-P-PDOT (**2**, Figure 1). New selective ligands might be developed as new therapeutic options for pathologies in which MT₁ or MT₂ have a relevant role.

Our studies on melatonin receptor ligands have led to the synthesis of several classes of compounds, among which N-anilinoethylamides are characterized by pharmacodynamic and metabolic profiles that could be finely tuned by proper scaffold decoration.^{9,10,11} UCM765 (**3**, Figure 1) is an MT₂ partial agonist which selectively promotes non-rapid eye movement sleep and exerts anxiolytic effects in rodents.^{12,13} Starting from these highly flexible ligands we devised a series of 2-acylaminomethyl-tetrahydroquinolines as conformationally-constrained, closed analog of the N-anilinoethylamide structure (Figure 2).¹⁴ Insertion of the tetrahydroquinoline (THQ) scaffold afforded potent compounds, with predictable structure-activity relationships (SAR) based on superposition models with known melatonin ligands. UCM1014 (**4**, Figure 1) is an MT₂ full agonist with remarkable selectivity for this receptor subtype (more than 10000-fold MT₂/MT₁ selectivity). Interestingly, high binding affinities could be obtained also for 2-acylaminomethylTHQs lacking the methoxy group,¹⁴ which is a metabolically liable substituent. In fact, cytochrome-catalyzed demethylation has been observed for melatonin receptor ligands characterized by different scaffolds.¹⁵ For aniline derivatives,

in particular, this was the major route of metabolic inactivation.¹⁰ Given the positive results obtained for 2-acylaminomethyl-THQs, we tested the possibility to get new melatonin receptor ligands with different patterns of substitution on the THQ scaffold. In particular, we i) explored the class of 3-acylaminomethyl-THQs by preparing a series of derivatives with different substituents on the nitrogen atom and in position 4 of the THQ ring and ii) compared the behavior of THQs with that of the corresponding tetralin analogues to evaluate if the THQ scaffold can be considered as a valuable bioisostere of the tetralin ring present in some of the best known and most characterized MT₁/MT₂ ligands (e.g., 4-P-PDOT, **2** in Figure 1). This would allow to extend the chemical space of melatonin receptor ligands, going toward more polar compounds that may improve the solubility and metabolism liabilities of the reference compounds employed so far, at least as far as they are related to high lipophilicity.

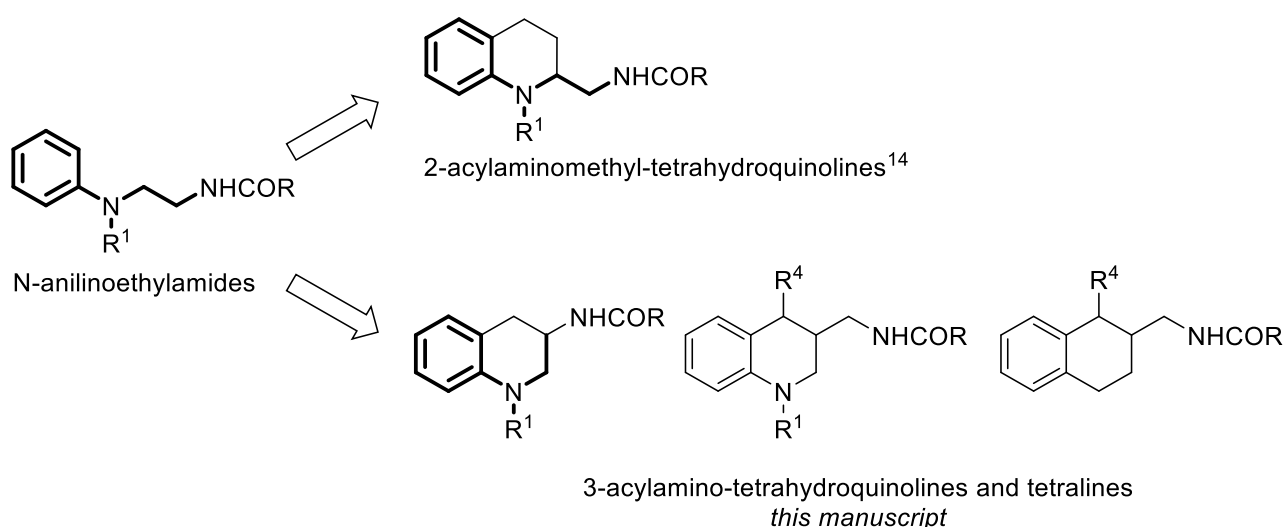
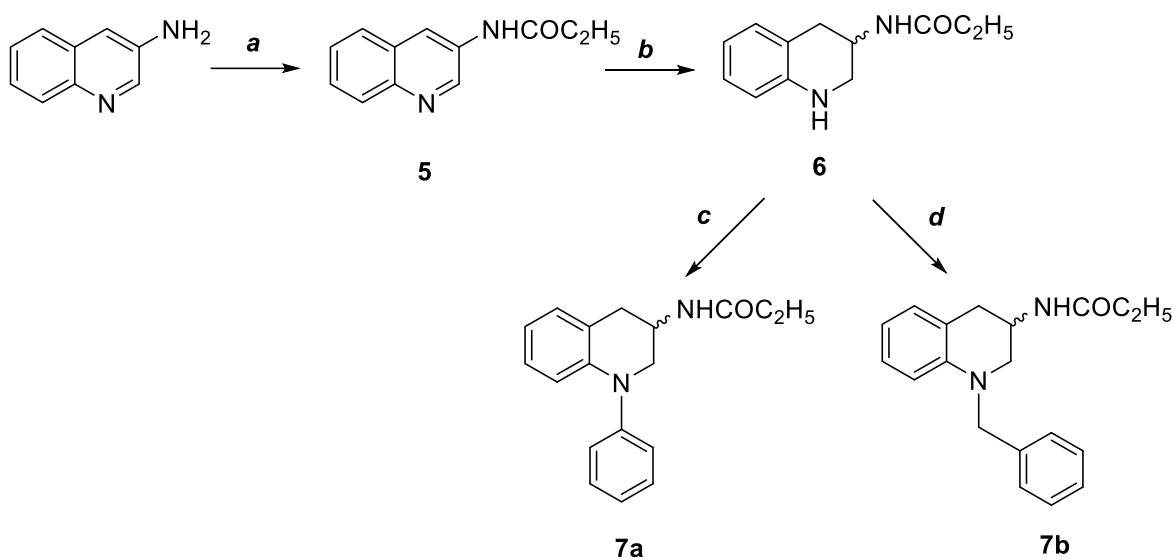


Figure 2. Schematic representation of tetrahydroquinoline melatonin receptor ligands and tetralin analogs.

Chemistry

Key intermediate for the synthesis of the 3-propionamidotetrahydroquinolines **7a-b** (Scheme 1) was 3-propionamidotetrahydroquinoline (**6**)¹⁶ that was obtained by *N*-acylation of the commercially available 3-aminoquinoline with propionic anhydride and subsequent reduction of the pyridine ring with NaBH₃CN/AcOH. The *N*-phenyl (**7a**) and *N*-benzyl (**7b**) target compounds were respectively prepared by palladium-catalyzed *N*-aryl amination or *N*-benzylation of **6**.

Scheme 1^a

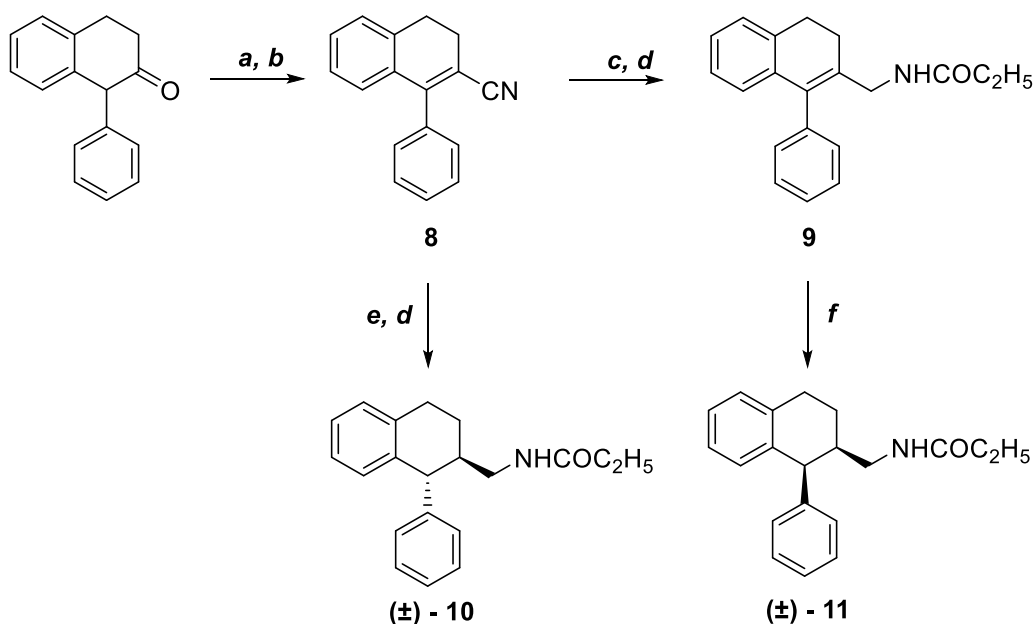


^aReagents and conditions: a) propionic anhydride, Et₃N, THF, reflux, 3 h, yield 81%; b) NaBH₃CN, AcOH, 50 °C → rt, 20 h, yield 40%; c) bromobenzene, Pd(OAc)₂, (±)-BINAP, *t*-BuOK, toluene, 100 °C, 6 h, yield 46%; d) benzyl bromide, Et₃N, toluene, reflux, 1 h, yield 61%.

The synthetic route adopted for the preparation of tetralin derivatives **9-11** is depicted in Scheme 2. The first step involved the reaction of 1-phenyl-3,4-dihydronaphthalen-2(1*H*)-one¹⁷ with

trimethylsilyl cyanide and ZnI_2 followed by treatment with phosphorus oxychloride in pyridine to give the intermediate nitrile **8** which was converted into the dihydronaphthalene derivative **9** by reduction with $\text{LiAlH}_4/\text{AlCl}_3$ and subsequent *N*-acylation of the crude intermediate amine with propionic anhydride. The *trans*-(**10**) and *cis*-(**11**) tetralin target compounds were respectively obtained by reduction of the unsaturated nitrile **8** with LiAlH_4 followed by *N*-acylation with propionic anhydride or by Pd-catalyzed hydrogenation of **9**.

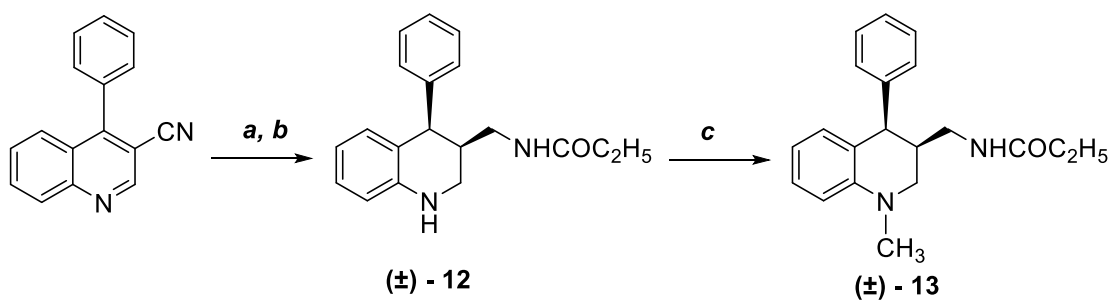
Scheme 2^a



^aReagents and conditions: a) trimethylsilyl cyanide, ZnI_2 , toluene, rt, 18 h; b) POCl_3 , Py, reflux, 1 h, two steps (a, b) yield 65%; c) $\text{LiAlH}_4/\text{AlCl}_3$, dry THF, rt, 1h; d) propionic anhydride, Et_3N , THF, rt, 16 h, two steps (c, d) yield 37%; e) LiAlH_4 , THF, reflux, 2 h, two steps (d, e) yield 30%; f) H_2 (4 atm), 10% Pd-C, MeOH, 60 °C, 6 h, yield 47%.

The 4-phenyl-tetrahydroquinoline derivative **12** was prepared by hydrogenation of 4-phenylquinoline-3-carbonitrile¹⁸ in the presence of Raney-Ni and subsequent *N*-acylation of the intermediate methanamine with propionic anhydride. The tetrahydroquinoline derivative **12** was then converted to the corresponding *N*¹-methyl derivative **13** by reductive amination with 37% HCHO, NaBH₃CN (Scheme 3).

Scheme 3^a

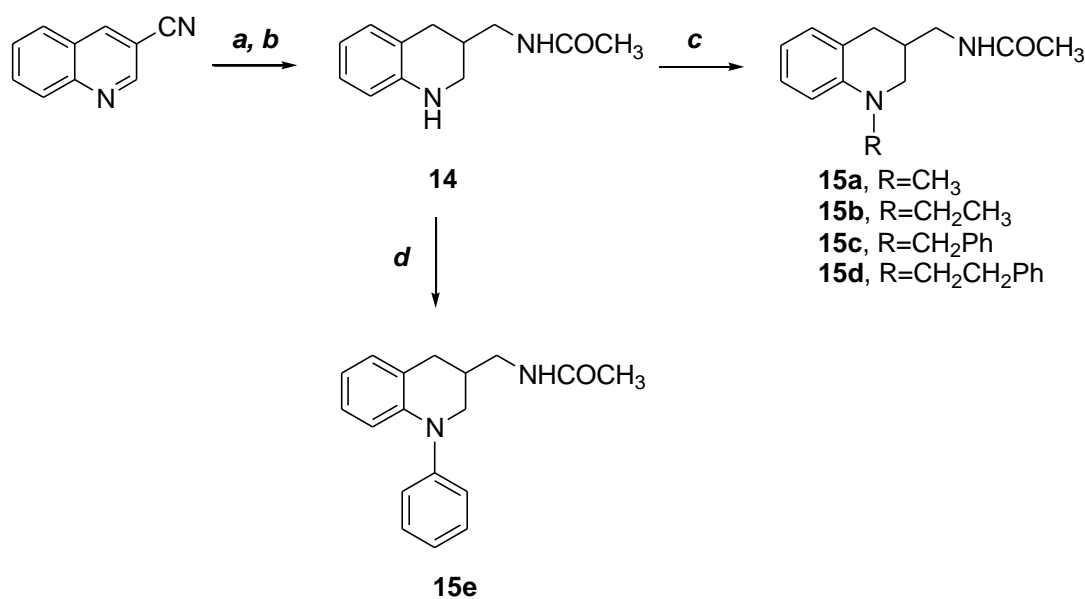


^aReagents and conditions: a) H₂ (4 atm), Raney-Ni, 2M NH₃ in EtOH, THF, 40 °C, 12 h; b) propionic anhydride, Et₃N, THF, rt, 1 h, two steps (a, b) yield 46%; c) 37% HCHO, NaBH₃CN, MeOH/AcOH, 40 °C, 3 h, yield 72%.

3-Methanamidotetrahydroquinoline **14** (Scheme 4) was prepared by hydrogenation (4 atm, 60 °C) of commercially available 3-cyanoquinoline in the presence of Raney-Ni and ammonia (a contemporary reduction of the nitrile and pyridine ring occurs), followed by *N*-acetylation of the intermediate primary methanamine. *N*¹-substituted 3-methanamido derivatives **15a-e** were prepared by *N*¹-alkylation of **14** with the suitable alkyl halide (**15a-d**) or by palladium-catalyzed *N*¹-arylation (**15e**)

using bromobenzene, palladium (II) acetate and [2,2'-bis-(diphenylphosphino)-1,1'-binaphthyl] (BINAP) (Scheme 4).

Scheme 4^a



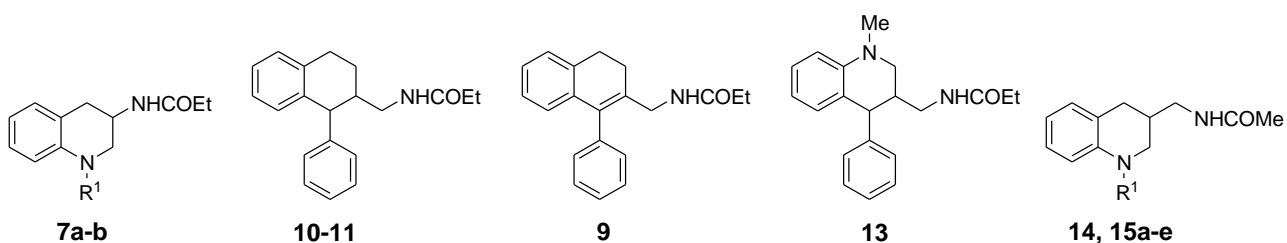
^aReagents and conditions: a) H₂ (4 atm), Raney-Ni, 2M NH₃ in EtOH, THF, 60 °C, 16 h; b) Ac₂O, Et₃N, THF, rt, 1 h, two steps (a, b) yield 70%; c) R-X, Et₃N, toluene, Δ, 1-16 h, yield 46-85%; d) bromobenzene, Pd(OAc)₂, BINAP, *t*-BuOK, toluene, 100 °C, 24 h, yield 29%.

Results and discussion

Table 1 reports hMT₁ and hMT₂ binding affinity, agonist potency and intrinsic activity values of new and reference compounds. Chiral compounds were tested as racemic mixtures. The best characterized melatonin receptor ligands with a tetralin scaffold are 4-P-PDOT (**2**, Figure 1) and its derivatives.¹⁹ *Cis*-4-P-PDOT is about hundred times selective for the MT₂ receptor and behaves as an MT₂ partial

agonist.²⁰ The principal aim of our investigation was to assess if the THQ scaffold can actually mimic the function of the tetralin ring at the melatonin receptors. As a first step, we explored the potential of the classical isosteric CH/N replacement preparing the 3-propionylaminoTHQ derivative **7a**. This compound showed nanomolar affinity (K_i) and agonist potency (EC_{50}) ($MT_1 K_i = 22$ nM, $EC_{50} = 20$ nM; $MT_2 K_i = 2$ nM, $EC_{50} = 1$ nM) and it behaved as a partial agonist at the MT_2 receptor. Compared to *cis*-4-P-PDOT, it resulted less potent at MT_2 receptor and thus less MT_2 -selective, while affinity at MT_1 receptor and partial agonist behavior were conserved. The *N*-benzyl substituent of compound **7b** ($MT_1 K_i = 892$ nM; $MT_2 K_i = 6$ nM, $EC_{50} = >10000$ nM) restored MT_2 selectivity and shifted intrinsic activity toward antagonism. This is consistent with the greater hindrance of the benzyl group in a region of the receptor binding site located out of the plane defined by the THQ nucleus. Occupation of this region has been proposed as one of the major determinants for MT_2 selectivity and limited intrinsic activity.²¹ Thus, for the 3-propionamido derivatives, bioisosterism between the tetralin and THQ scaffolds was confirmed.

Table 1. Binding Affinity, Agonist Potency and Intrinsic Activity of 3-Acylaminotetrahydroquinoline and Tetralin Derivatives at Human MT_1 and MT_2 Melatonin Receptors^a



Compd. ^b	R ¹	MT ₁	MT ₂	MT ₂ -Selectivity
---------------------	----------------	-----------------	-----------------	------------------------------

		K_i (nM)	EC₅₀ (nM)	E_{max} (%)	K_i (nM)	EC₅₀ (nM)	E_{max} (%)	
1 (MLT)^c		0.23 [0.21;0.26]	1.7 [1.1;2.5]	123±13	0.52 [0.40;0.58]	0.4 [0.3;0.6]	76±6	0.4
2 (cis-4-P-PDOT)^d		76 [46;126]		23±6	0.69 [0.60;0.79]		46±2	110
7a	Ph	22 [16;33]	20 [15;29]	29±3	2 [1;4]	1 [1;2]	41±3	11
7b	Bn	892 [553;1440]			6 [3.5;11]	> 10000		149
9		28 [22;34]		16±8	3.8 [3.3;4.3]		30±6	7.4
10 (trans)		62 [28;136]		61±4	0.23 [0.20;0.26]		78±9	270
11 (cis)		3.5 [2.3;5.2]		56±8	0.22 [0.18;0.28]		75±3	16
cis-13		3.4 [3.2; .6]		82±7	0.48 [0.46;0.49]		75±3	7.1
14	H	430 [210;881]			110 [62;194]			3.9
15a	Me	83 [54;128]	> 10000		15 [8;28]	10 [5;34]	32±6	5.5
15b	Et	20 [14;28]	> 10000		1 [0.2;3]	7 [3;17]	59±8	20
15c	Bn	59 [25;140]			1 [0.8;2]	3 [2;4]	28±4	59
15d	Phenethyl	246 [136;445]			47 [34;65]	80 [76;94]	47±5	5.2

15e	Ph	3 [1;4]	> 10000		0.3 [0.2;0.4]	> 10000		10
------------	----	------------	---------	--	------------------	---------	--	----

^a K_i and EC_{50} (nM) values are geometric mean values (with 95% confidence limits shown in brackets) of at least two separate experiments performed in duplicate. E_{max} values are arithmetic mean values \pm SEM. ^bChiral compounds were tested as racemates. ^cTaken from ref. 22. ^dTaken from ref. 20.

As discussed in the Introduction, an excellent class of THQ melatonin receptor ligands is that of 2-acylaminomethyl-THQs, in which the amide side chain is linked to the tetralin scaffold through a methylene bridge (Figure 2).¹⁴ According to pharmacophore models previously developed by us, the THQ ring is not involved in polar interactions with the receptor binding site. For this reason we thought that, also in this case, the THQ nitrogen atom could simply mimic a CH group. To evaluate this hypothesis, we prepared the two *trans*- and *cis*-1-phenyltetralin diastereoisomers **10** and **11**, respectively, and investigated their preferred conformational states. The conformational equilibrium of compounds **10** and **11** was firstly simulated by means of metadynamics runs, following a protocol previously applied to similar compounds.¹⁴ Briefly, the compounds were solvated into a water box and the two dihedral angles τ_1 and τ_2 were used as the collective variables to deposit biasing potentials that force the exploration of the conformational space. τ_1 and τ_2 (Figure 3a) describe the conformation of the THQ ring and the orientation of the amide side chain, respectively.

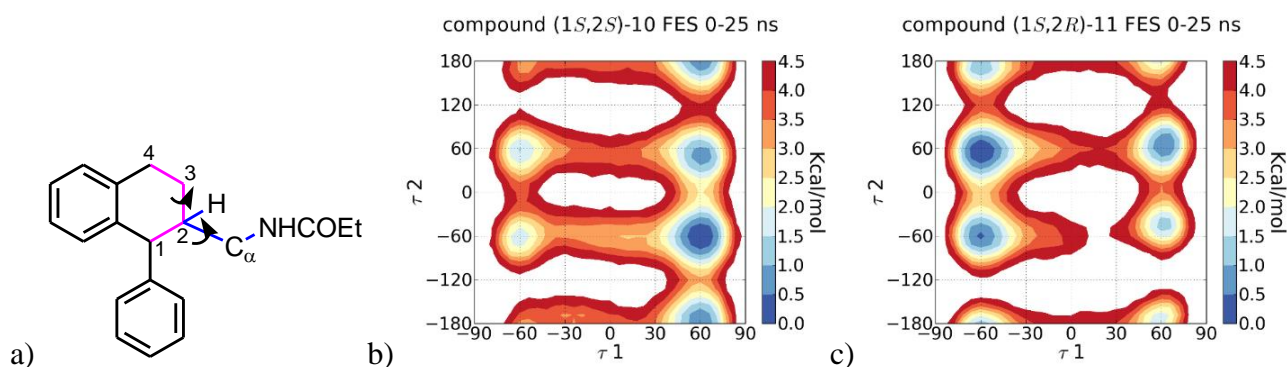


Figure 3. a) Representation of τ_1 ($C_1-C_2-C_3-C_4$, pink bonds) and τ_2 ($H_2-C_2-C_\alpha-N$, blue bonds) dihedral angles. b and c) Free energy surfaces for compounds (1*S*,2*S*)-**10** (b) and (1*S*,2*R*)-**11** (c) obtained after 25 ns of well-tempered metadynamics simulations.

Free energy surface (FES) calculated for one enantiomer of the *trans* isomer **10** (Figure 3b) highlighted the preference for a *trans*-diequatorial arrangement of the two substituents ($\tau_1 \sim 60^\circ$ for the 1*S*,2*S* enantiomer). The amide side chain is free to rotate, with three free energy minima corresponding to τ_2 values around 60, 180 and -60° . ^1H NMR spectrum showed vicinal coupling constants between H^2 and the two distinct H^3 protons of 9.0 and 3.0, which is consistent with a prevalent conformation of the tetralin ring with H^2 in an axial arrangement. This confirms the diequatorial conformation of the two substituents (see Supporting Information Figure S1 and Table S1 for complete assignment of chemical shifts, geminal and vicinal coupling constants). The metadynamics simulation for compound **11** revealed an equilibrium between the equatorial ($\tau_1 \sim 60^\circ$ for the 1*S*,2*R* enantiomer) and the axial arrangement ($\tau_1 \sim 60^\circ$) of the side chain, with a small difference in energy content between the two (about 0.6 kcal/mol, Figure 3c). The side chain is free to rotate with τ_2 minima located at the typical values of -60 , 180 and 60° . In fact, NMR spectrum of compound **11** shows a mixture of axial and equatorial amide side chain. In particular, $J_{2-3a} = 6.5$ Hz originates from the combination of a *gauche* and an *anti* arrangement of the two protons while $J_{2-3e} = 3.5$ Hz derives from two *gauche* arrangements (see Supporting Information Figure S2 and Table S2 for complete NMR data).

A major difference between the 1,2-disubstituted THQ and tetralin derivatives is that the last scaffold presents *trans*- and *cis*- isomerism, while the first allows nitrogen inversion, which leads to a single

couple of enantiomers with the *N*-substituent only influencing the conformational arrangement of the side chain in position 2.¹⁴ The THQ derivative corresponding to **10** and **11** is a sub-nanomolar MT₂ agonist ($K_i = 0.06$ nM, $E_{\max} = 90\%$) with moderate selectivity toward the MT₁ subtype ($K_i = 1.6$ nM, $E_{\max} = 69\%$).¹⁴

The *trans* isomer **10** in its diequatorial conformation can be closely superposed to the bioactive conformation of melatonin (Figure 4a). The aromatic portion of the tetralin ring is positioned in the same region as the benzene of the indole of MLT and the amide groups point in the same direction. The phenyl substituent occupies the out-of-plane region related to selectivity for the MT₂ receptor. Consistently with its shape, compound **10** (MT₁ $K_i = 62$ nM; MT₂ $K_i = 0.23$ nM) is a potent and selective (~300 times) MT₂ partial agonist. The *cis* isomer **11** (MT₁ $K_i = 3.5$ nM; MT₂ $K_i = 0.22$ nM) can also be superposed to melatonin with an equatorial arrangement of its side chain (Figure 4a). This can account for its high affinity at the MT₂ receptor subtype. However, this compound shows higher MT₁ binding affinity, and thus lower selectivity, than **10**. The binding mode depicted in Figure 4a is in contrast with this behavior, since the axial phenyl ring would be accommodated in the out-of-plane region hampered at the MT₁ receptor. One possible explanation for its lower selectivity is that compound **11** can also be superposed to melatonin with its side chain in axial conformation (Figure 4b), which allows to position the phenyl ring in a region which corresponds to position 2 of the melatonin ring, allowed for both receptor subtypes.

Partial unsaturation of the tetralin scaffold (**9**) unexpectedly led to a significant reduction of MT₂ affinity, and of selectivity, compared to the *trans* isomer **10**. While this is in apparent contrast with the diequatorial-like arrangement of its substituents, conjugation with the double bond affects the conformational space of the phenyl ring, and this may be the cause for lower MT₂ affinity.

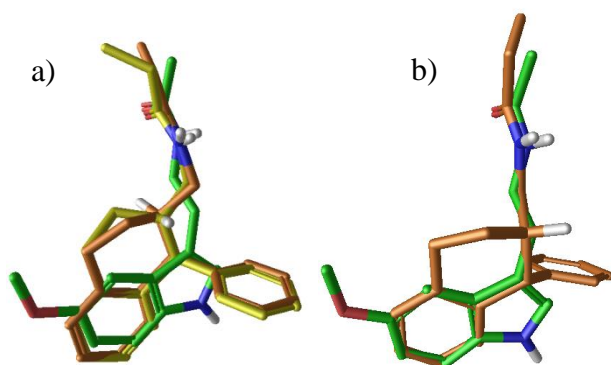


Figure 4. a) Superposition of the bioactive conformation of melatonin (green carbons) with compound **10** (yellow carbons) and compound **11** (orange carbons) with equatorial arrangement of its side chain. b) Superposition of melatonin and compound **11** with axial arrangement of its side chain.

Thus, also for 1-phenyl-2-acylaminomethyl derivatives, THQ and tetralin scaffolds can give similar binding profiles at melatonin receptors. To put forward the comparison, we explored the possibility to apply another isosteric CH/N replacement at the atom opposite to the one carrying the phenyl ring. This resulted in the synthesis of compound **13**, a THQ derivative having a phenyl ring in position 4, and the acylaminomethyl side chain in position 3. With the synthetic route applied we only obtained the racemic mixture of the *cis* isomers. NMR analysis demonstrated the *cis* configuration of the 3,4-disubstituted THQ, given the small coupling constant calculated for protons 3 and 4 ($J_{3-4} \sim 5.0$ Hz). The phenyl ring is in pseudo-axial position and the amide chain has equatorial arrangement, as confirmed from the large coupling constant J_{2a-3} (~ 11.5 Hz) and the small one J_{2e-3} (~ 4.0 Hz). Additionally, a small constant for the long range W coupling between protons 2e and 4 could be measured (${}^4J_{2e-4} \sim 1.0$ Hz), consistent with the axial arrangement of the phenyl ring. In the 2D-NOESY spectrum the cross-peak observed between proton 2a and the hydrogens of the phenyl ring is only

compatible with a pseudo-axial arrangement of the phenyl substituent (see Supporting Information Figures S3 and S4 and Table S3 for complete data and spectra).

While affinity and intrinsic activity data for *cis*-**13** ($MT_1 K_i = 3.4$ nM; $MT_2 K_i = 0.48$ nM), very similar to those of the *cis*-substituted tetralin **11**, further confirmed the bioisosterism between the two series, its NMR spectra clearly show a different conformational behavior. In particular, the equatorial arrangement of its side chain rules out the explanation proposed for the reduced subtype selectivity of **11**, which was attributed to a conformational equilibrium between axial and equatorial arrangements. As the superposition of the preferred conformation of *cis*-**13** placed its axial phenyl ring in the position occupied by the phenyl of compound **11**, which is considered forbidden at MT_1 receptor (Figure 5a), the accommodation of *cis*-**13** within the MT_1 binding site could be different, flipping around the THQ nucleus and leaving the MT_1 -forbidden region empty (Figure 5b).

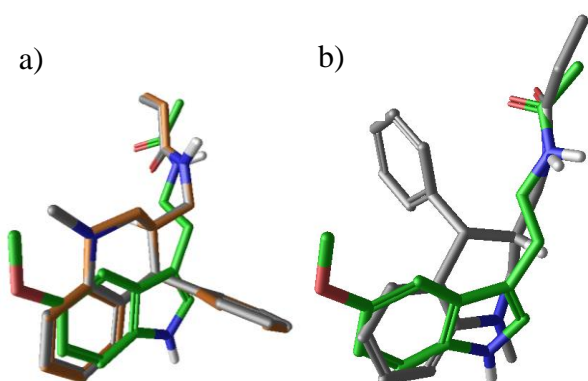


Figure 5. a) Superposition of melatonin (green carbons), compound *cis*-**13** (gray carbons) and **11** (yellow carbons). b) Superposition of melatonin and compound *cis*-**13** in the alternative orientation discussed in the text.

Compound **13** also introduces a new application of the design of melatonin ligands based on the THQ scaffold. According to the superposition represented in Figure 5b, 3-acylaminomethyl-THQs should

allow substitution at nitrogen with groups that can be accommodated in allowed regions of the MT₁ and, particularly, MT₂ binding sites. We therefore prepared compounds **14** and **15a-e** in which we investigated the influence on receptor activity of the size and shape of the substituent on the THQ nitrogen atom. The presence of an alkyl substituent significantly improved MT₁ and MT₂ binding affinity, with a 5 to 10-fold increase in potency for the N-methyl derivative (**15a**) compared to the N-unsubstituted one (**14**). The potency of the compounds was roughly correlated with the size of the substituent. In fact, moving from methyl (**15a**) to ethyl (**15b**) to phenyl (**15e**), nanomolar and subnanomolar binding affinities could be reached. In particular, the N-phenyl derivative **15e** had similar MT₁ and MT₂ binding affinities to 4-phenyl-THQ **13** and the tetralin analog **11**. The N-benzyl derivative **15c** had higher MT₂-selectivity, as already observed for compounds with out-of-plane substituents. NMR investigations of **15e** pointed out that the acylaminomethyl side chain has an equatorial arrangement which allows a good superposition with melatonin (Figure 6). *J* values for proton H₃ with the two distinct H₂ protons (H_{2a} and H_{2e}; *J* = 10.0 and 4.5 Hz, respectively) are consistent with a fixed arrangement of the THQ nucleus, with H₃ *anti* to H_{2a}. NOE contact between H_{2a} and H_{4a} is in line with this arrangement with equatorial side chain (see Supplementary Material Figure S5, S6 and Table S4 for spectra and complete data). Similar NMR patterns, supporting equatorial amide side chain conformations, were recorded for the other 3-acylaminomethylTHQs **14** and **15b-d**.

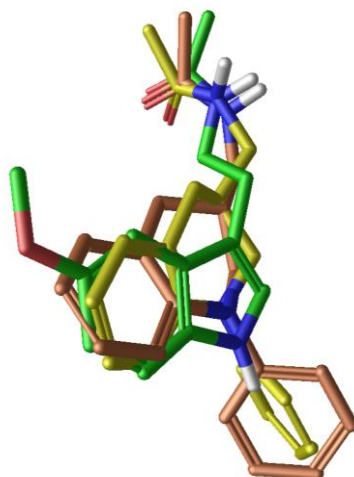


Figure 6. Superposition of melatonin (green carbons) and the enantiomers of compound **15e**.

Since stereoselectivity is known to play a role for melatonin receptor ligands,²³ to investigate the influence of chirality on the interaction of these derivatives with the receptor, the chiral resolution of the potent compound **15e** was performed. Briefly, on the basis of our previous experience the racemate **15e** was resolved by chiral high-performance liquid chromatography (HPLC), this approach being an effective way for both the analytical and the preparative separations of chiral compounds.^{24,25} A proper chiral resolution method was set up in analytical scale, and then it was suitably scaled-up to (semi)-preparative scale, allowing to obtain both enantiomers of **15e** in good yields and high enantiomeric excess.

Binding affinity and intrinsic activity of (+)- and (-)-**15e** were evaluated and are reported in Table 2. The enantiomers displayed similar potencies and intrinsic activities at both receptors, likely due to the equatorial arrangement of the acetylaminomethyl side chain, which allows good superposition of each enantiomer to the putative active conformation of melatonin (Figure 6).

Table 2. Binding Affinity and Intrinsic Activity of Enantiomers of Compound **15e** at Human MT₁ and MT₂ Melatonin Receptors.^a

Compd. ^b	MT ₁		MT ₂	
	K _i (nM)	E _{max} (%)	K _i (nM)	E _{max} (%)
(±)- 15e	2.4 [2.21;2.61]	27±9	1.2 [1.09;1.33]	10±1
(-)- 15e	3.02 [2.45;3.72]	30±8	1.38 [1.16;1.64]	29±2
(+)- 15e	1.58 [1.2;2.09]	25±9	0.78 [0.61;0.99]	5±3

^aK_i values are geometric mean values (with 95% confidence limits shown in brackets) of at least two separate experiments performed in duplicate. E_{max} values are arithmetic mean values ± SEM.

Summarizing the observed SARs, MT₂ binding affinity is very high when an aromatic substituent is close to the amide side chain (1,2 substitution) for both tetralin and THQ derivatives (e.g., compounds **10**, **11** and **13**), which is consistent with the remarkable affinity previously observed for 2-acylaminoethylTHQ derivatives. However, the versatility of the THQ scaffold allowed to achieve sub-nanomolar MT₂ binding affinity also for compound **15e**, having 1,3 substitution pattern.

Conclusions

3-Acylamino-THQ derivatives were prepared as conformationally-constrained analogues of flexible N-anilinoethylamide melatonin ligands. Even if newly synthesized compounds do not reach the remarkable affinity and MT₂ selectivity of a previously described THQ derivative, i.e., compound **4**, they prove that the THQ nucleus is a synthetically accessible scaffold for melatonin receptor ligands, endowed with peculiar versatility. We demonstrated that THQ derivatives can mimic the SARs observed for tetralin ones (e.g., 4-P-PDOT) and vice versa, avoiding the presence of the aromatic methoxy group which, in some melatonergic agents, is responsible for low metabolic stability. The

THQ scaffold has higher polarity and lacks one stereocenter, compared to the tetralin one. It was also possible to obtain potent melatonin ligands with different topology, belonging to the class of 3-acylaminomethyl-THQs, which was suggested by alternative accommodations of the ligands within the binding site, all of them fulfilling the pharmacophore requirements for proper receptor binding.

Experimental section

General procedures

Melting points were determined on a Buchi B-540 capillary melting point apparatus and are uncorrected. ^1H NMR and ^{13}C NMR spectra were recorded on a Bruker AVANCE 200 or 400 instrument. Chemical shifts (δ scale) are reported in parts per million (ppm) relative to the central peak of the solvent. Coupling constants (J) are given in hertz (Hz). ^1H and ^{13}C signals were unambiguously assigned by COSY, NOESY, DEPT135, HMQC and HMBC experiments. EI MS spectra (70 eV) were taken on a Fisons Trio 1000 instrument; only molecular ions (M^+) and base peaks are given. ESI MS spectra were taken on a Waters Micromass ZQ instrument; only molecular ions ($\text{M}+1$)⁺ are given. High-resolution mass spectroscopy was performed on a Micromass Q-ToF Micro mass spectrometer (Micromass, Manchester, UK) using an ESI source. The purity of tested compounds, determined by high pressure liquid chromatography (HPLC), was greater than 95% (Supporting Information Table S5). These analyses were performed on a Waters HPLC/UV/MS system (separation module Alliance HT2795, Photo Diode Array Detector 2996, mass detector Micromass ZQ; software: MassLynx 4.1). Column chromatography purifications were performed under “flash” conditions using Merck 230–400 mesh silica gel. Analytical thin-layer chromatography (TLC) was carried out on Merck silica gel 60 F254 plates.

Chiral HPLC runs were conducted on a Jasco (Cremella, LC, Italy) HPLC system equipped with a Jasco AS-2055 plus autosampler, a PU-2089 plus quaternary gradient pump, and an MD-2010 plus

multi-wavelength detector. Experimental data were acquired and processed by Jasco Borwin PDA and Borwin Chromatograph Software. Solvents used for chiral chromatography were HPLC grade and supplied by Carlo Erba (Milan, Italy). Optical rotation values were measured on a Jasco (Cremella, LC, Italy) photoelectric polarimeter DIP 1000 with a 0.2 dm cell at the sodium D line ($\lambda=589$ nm); sample concentration values (c) are given in 10^{-2} g mL⁻¹.

3-Quinolinecarbonitrile and 3-aminoquinoline were purchased from commercial suppliers and used without further purification.

***N*-(Quinolin-3-yl)propionamide (5)**. A solution of 3-aminoquinoline (1 g, 7 mmol), Et₃N (1.53 mL, 11 mmol) and propionic anhydride (0.9 mL, 7 mmol) in THF (30 mL) was heated at reflux for 3 h. After removing the solvent by distillation under reduced pressure, the residue was taken up in CH₂Cl₂, washed twice with 2N NaOH, once with brine and dried (Na₂SO₄). The solvent was removed under reduced pressure and the crude residue was purified by crystallization. White solid, mp 167-8 °C (CH₂Cl₂-petroleum ether); 81% yield. ¹H NMR (200 MHz, DMSO-*d*₆): δ 1.12 (t, 3H, *J* = 7.5 Hz), 2.43 (q, 2H, *J* = 7.5 Hz), 7.50-7.65 (m, 2H), 7.86-7.95 (m, 2H), 8.70 (s, 1H), 8.92 (s, 1H), 10.57 (s, 1H). EI MS (*m/z*): 200 (M⁺), 144 (100).

(±)-*N*-(1,2,3,4-Tetrahydroquinolin-3-yl)propionamide (6).¹⁶ NaBH₃CN (0.265 g, 4.2 mmol) was added portion wise during 5 min to a solution of *N*-(quinolin-3-yl)propionamide **5** (0.2 g, 1 mmol) in AcOH (3 mL) and the resulting mixture was stirred at room temperature for 1 h, at 50 °C for 1 h and finally at room temperature for 18 h. The reaction mixture was quenched with water, adjusted to pH 11 by adding 30% NaOH, and the aqueous phase was extracted with CH₂Cl₂ (3x). The combined organic layers were dried (Na₂SO₄) and concentrated under reduced pressure to afford a crude residue which was purified by silica gel flash chromatography (CH₂Cl₂-EtOAc 6:4 as eluent) and crystallization. White solid, mp 90-1 °C (diethyl ether-petroleum ether); 40% yield. ¹H NMR (200

MHz, CDCl₃): δ 1.12 (t, 3H, $J = 7.5$ Hz), 2.17 (q, 2H, $J = 7.5$ Hz), 2.74 (ddd, 1H, $J_1 = 2.0$, $J_2 = 3.5$, $J_3 = 16.5$ Hz), 3.08 (dd, 1H, $J_1 = 5.0$, $J_2 = 16.5$ Hz), 3.22 (ddd, 1H, $J_1 = 2.0$, $J_2 = 4.0$, $J_3 = 11.5$ Hz), 3.39 (dd, 1H, $J_1 = 2.5$, $J_2 = 11.5$ Hz), 3.94 (brs, 1H), 4.44-4.56 (m, 1H), 5.95 (brs, 1H), 6.55 (dd, 1H, $J_1 = 1.0$, $J_2 = 8.0$ Hz), 6.69 (ddd, 1H, $J_1 = 1.0$, $J_2 = J_3 = 7.5$ Hz), 6.96-7.08, (m, 2H). EI MS (m/z): 204 (M^+), 130 (100).

(\pm)-*N*-(1-Phenyl-1,2,3,4-tetrahydroquinolin-3-yl)propionamide (7a). A Schlenk flask was charged with Pd(OAc)₂ (22 mg, 0.1 mmol), (\pm)-BINAP (60 mg, 0.1 mmol), *t*-BuOK (0.26 g, 2.32 mmol) and **6** (0.204 g, 1 mmol) in dry toluene (2 mL) under nitrogen atmosphere. Bromobenzene (0.2 mL, 2 mmol) was added dropwise via syringe and the resulting mixture was stirred at 100 °C for 6 h. After cooling to room temperature the reaction mixture was quenched with water and then extracted twice with CH₂Cl₂. The combined organic phases were dried over Na₂SO₄ and concentrated by distillation under reduced pressure to yield a crude residue that was purified by silica gel flash chromatography (cyclohexane-EtOAc 3:7 as eluent) and crystallization. Beige solid, mp 163-4 °C (CH₂Cl₂-petroleum ether); 46% yield. ¹H NMR (200 MHz, CDCl₃): δ 1.09 (t, 3H, $J = 7.5$ Hz), 2.14 (q, 2H, $J = 7.5$ Hz), 2.83 (ddd, 1H, $J_1 = 2.0$, $J_2 = 3.5$, $J_3 = 16.5$ Hz), 3.22 (dd, 1H, $J_1 = 5.5$, $J_2 = 16.5$ Hz), 3.59 (ddd, 1H, $J_1 = 2.0$, $J_2 = 4.5$, $J_3 = 11.5$ Hz), 3.76 (dd, 1H, $J_1 = 2.5$, $J_2 = 11.5$ Hz), 4.53-4.63 (m, 1H), 5.79 (brs, 1H), 6.71-6.80 (m, 2H), 6.94-7.44 (m, 7H). ¹³C NMR (100 MHz, CDCl₃): δ 173.3, 147.4, 143.9, 130.5, 129.7, 126.9, 125.2, 124.7, 120.3, 118.9, 115.1, 54.0, 42.7, 33.4, 29.7, 9.7. EI MS (m/z): 280 (M^+), 206 (100). HRMS (ESI): m/z calculated for C₁₈H₂₀N₂O, [M + H]⁺ 281.1654. Found: 281.1631.

(\pm)-*N*-(1-Benzyl-1,2,3,4-tetrahydroquinolin-3-yl)propionamide (7b). A solution of **6** (0.204 g, 1 mmol), Et₃N (0.8 mL, 5.7 mmol) and benzyl bromide (5 mmol) in dry toluene (6 mL) was heated for 1 h under reflux. After cooling to room temperature, the reaction mixture was poured into water, extracted with EtOAc (4x), and the combined organic phases were washed with brine and dried

(Na₂SO₄). The solvent was removed by distillation *in vacuo* and the residue was purified by silica gel flash chromatography (cyclohexane-EtOAc 3:7 as eluent) and crystallization. Beige solid, mp 132-3 °C (CH₂Cl₂-petroleum ether); yield 61%. ¹H NMR (400 MHz, DMSO-*d*₆): δ 0.99 (t, 3H, *J* = 7.5 Hz), 2.10 (q, 2H, *J* = 7.5 Hz), 2.69 (dd, 1H, *J*₁ = 9.0, *J*₂ = 15.5 Hz), 2.93 (ddd, 1H, *J*₁ = 1.5, *J*₂ = 4.5, *J*₃ = 15.5 Hz), 3.17 (dd, 1H, *J*₁ = 8.5, *J*₂ = 11.0 Hz), 3.40 (ddd, 1H, *J*₁ = 1.5, *J*₂ = 4.0, *J*₃ = 11.0 Hz), 4.13 (dddd, 1H, *J*₁ = 4.0, *J*₂ = 4.5, *J*₃ = 8.5, *J*₄ = 9.0 Hz), 4.43 (d, 1H, *J* = 17.0 Hz), 4.53 (d, 1H, *J* = 17.0 Hz), 6.50-6.53 (m, 2H), 6.90-6.95 (m, 2H), 7.20-7.34 (m, 5H), 7.77 (d, 1H, *J* = 7.5 Hz). ¹³C NMR (100 MHz, CDCl₃): δ 173.4 (CO), 144.6, 138.3, 130.4, 128.7, 127.7, 127.1, 126.8, 118.6, 117.1, 111.5, 54.9 (C3), 53.2 (C2), 41.9 (CH₂Ph), 33.5 (C4), 29.7 (CH₂CH₃), 9.7 (CH₂CH₃). EI MS (*m/z*): 294 (M⁺), 220 (100). HRMS (ESI): *m/z* calculated for C₁₉H₂₂N₂O, [M + H]⁺ 295.1810. Found: 295.1810.

1-Phenyl-3,4-dihydronaphthalene-2-carbonitrile (8). A solution of 1-phenyl-3,4-dihydronaphthalen-2(1*H*)-one¹⁷ (1 g, 4.5 mmol), trimethylsilyl cyanide (0.8 mL, 6 mmol), and ZnI₂ (0.038 g, 0.11 mmol) in dry toluene (3.5 mL) was stirred at room temperature for 18 h. Pyridine (6 mL) and afterward POCl₃ (1.3 mL, 14 mmol) were added to the above solution, and the resulting mixture was refluxed for 1 h. After cooling to room temperature, the reaction mixture was poured into 5% HCl/ice and the aqueous phase was extracted with EtOAc. The combined organic extracts were washed with brine, dried (Na₂SO₄), and concentrated under reduced pressure to give a crude residue that was purified by flash chromatography (silica gel, cyclohexane-EtOAc 9:1 as eluent) and crystallization. White solid, mp 81-2 °C (diethyl ether-petroleum ether); 65% yield. ¹H NMR (200 MHz, CDCl₃): δ 2.64-2.73 (m, 2H), 2.95-2.99 (m, 2H), 6.86-7.51 (m, 9H). ESI MS (*m/z*): 232 (M+H)⁺.

***N*-[(1-Phenyl-3,4-dihydronaphthalen-2-yl)methyl]propionamide (9).** A suspension of aluminum trichloride (0.293 g, 2.2 mmol) in dry THF (2.8 mL) was added to a stirred ice-cooled suspension of LiAlH₄ (0.041 g, 1.1 mmol) in dry THF (1.3 mL) under a nitrogen atmosphere. The mixture was stirred for 10 min, a solution of the nitrile **8** (232 mg, 1.0 mmol) in dry THF (0.9 mL) was then added dropwise and the resulting mixture was stirred at room temperature for 2 h. Water was carefully added at 0 °C, and the resulting mixture was filtered through a Celite pad. The filtrate was concentrated *in vacuo*, and partitioned between water and EtOAc. The combined organic phases were washed with brine, dried (Na₂SO₄) and concentrated under reduced pressure to yield the crude desired amine which was used without any further purification. Et₃N (0.15 mL, 1.07 mmol) and propionic anhydride (0.136 mL, 1.07 mmol), were added to a stirred solution of the above crude amine in dry THF (12 mL) and the mixture was stirred at room temperature for 16 h. The solvent was evaporated *in vacuo*, and the residue was dissolved in EtOAc. The solution was washed with 2N NaOH, with brine, dried (Na₂SO₄) and then concentrated under reduced pressure to give a crude residue that was purified by flash chromatography (silica gel, cyclohexane-EtOAc 7:3 as eluent) and crystallization. White solid, mp 154-5 °C (EtOAc-petroleum ether); 37% yield. ¹H NMR (200 MHz, CDCl₃): δ 1.14 (t, 3H, *J* = 7.5 Hz), 2.19 (q, 2H, *J* = 7.5 Hz), 2.41-2.49 (m, 2H), 2.85-2.93 (m, 2H), 3.91 (d, 2H, *J* = 6.0 Hz), 5.29 (brt, 1H), 6.61 (dd, 1H, *J*₁ = 1.5, *J*₂ = 7.0 Hz), 7.00-7.19 (m, 5H), 7.35-7.49 (m, 3H). ¹³C NMR (100 MHz, CDCl₃): δ 173.7, 138.5, 136.8, 136.1, 135.3, 133.7, 129.9, 128.6, 127.2, 126.9, 126.2, 126.0, 42.1, 29.8, 28.3, 25.9, 9.9. ESI MS (*m/z*): 292 (M+H)⁺. HRMS (ESI): *m/z* calculated for C₂₀H₂₁NO, [M + H]⁺ 292.1701. Found: 292.1715.

(±)-*trans*-N-[(1-Phenyl-1,2,3,4-tetrahydronaphthalen-2-yl)methyl]propionamide (10). A solution of **8** (0.1 g, 0.43 mmol) in dry THF (1.5 mL) was added dropwise to a stirred ice-cooled suspension of LiAlH₄ (0.035 g, 0.92 mmol) in dry THF (0.5 mL) stirred under nitrogen atmosphere at 0 °C. The reaction mixture was refluxed for 2 h, quenched by water addition at 0 °C and then

filtered on Celite. The filtrate was extracted with EtOAc (3x) and the combined organic phases were dried (Na₂SO₄), and concentrated under reduced pressure to give the desired crude corresponding amine. Et₃N (0.08 mL, 0.57 mmol) and propionic anhydride (0.07 mL, 0.54 mmol) were added to a solution of the above crude amine in THF (5 mL), and the resulting mixture was stirred at room temperature for 16 h. After distillation of the solvent under reduced pressure, the residue was partitioned between EtOAc and 2N NaOH. The organic layer was washed with brine, dried (Na₂SO₄), and concentrated under reduced pressure to give a crude residue which was purified by flash chromatography (silica gel, CH₂Cl₂-acetone 95:5 as eluent) and crystallization. White solid, mp 120-1 °C (EtOAc-petroleum ether); 30% yield. ¹H NMR (400 MHz, MeOD): δ 1.11 (t, 3H, *J* = 7.5 Hz), 1.57 (dddd, 1H, *J*₁ = 6.5, *J*₂ = 8.5, *J*₃ = 9.0, *J*₄ = 13.5 Hz), 2.03 (dddd, 1H, *J*₁ = 3.0, *J*₂ = *J*₃ = 5.5, *J*₄ = 13.5 Hz), 2.14 (dddd, 1H, *J*₁ = 3.0, *J*₂ = 5.5, *J*₃ = *J*₄ = 8.0, *J*₅ = 9.0 Hz), 2.17 (q, 2H, *J* = 7.5 Hz), 2.87-2.99 (m, 2H), 3.14 (dd, 1H, *J*₁ = 5.5, *J*₂ = 13.5 Hz), 3.19 (dd, 1H, *J*₁ = 8.0, *J*₂ = 13.5 Hz), 3.84 (d, 1H, *J* = 8.0 Hz), 6.71 (d, 1H, *J* = 8.0 Hz), 6.98 (ddd, 1H, *J*₁ = 1.5, *J*₂ = *J*₃ = 8.0 Hz), 7.06-7.14 (m, 4H), 7.20 (dddd, 1H, *J*₁ = *J*₂ = 1.5, *J*₃ = *J*₄ = 7.5 Hz), 7.27-7.31 (m, 2H). ¹³C NMR (100 MHz, CDCl₃): δ 173.8 (CO), 145.8, 139.0, 136.6, 130.2, 129.3, 128.6, 126.5, 125.93, 125.89, 50.7 (C1), 43.7 (C2), 42.8 (C11), 29.6 (C4), 28.8 (CH₂CH₃), 26.2 (C3), 9.8 (CH₂CH₃). ESI MS (*m/z*): 294 (M+1)⁺. HRMS (ESI): *m/z* calculated for C₂₀H₂₃NO, [M + H]⁺ 294.1858. Found: 294.1858.

(±)-*cis*-N-[(1-Phenyl-1,2,3,4-tetrahydronaphthalen-2-yl)methyl]propionamide (11). A solution of **9** (0.3 g, 1.3 mmol) in MeOH (6 mL) was hydrogenated (4 atm) in the presence of 10% Pd/C for 6 h at 60 °C. The catalyst was removed by filtration on Celite and the filtrate evaporated under reduced pressure to afford a crude product which was purified by flash chromatography (silica gel, CH₂Cl₂-acetone 95:5 as eluent) and crystallization. White solid, mp 129-30 °C (diethyl ether-petroleum ether);

47% yield. ^1H NMR (400 MHz, DMSO- d_6): δ 0.99 (t, 3H, $J = 7.5$ Hz), 1.51 (dddd, 1H, $J_1 = 6.0$, $J_2 = 6.5$, $J_3 = 11.5$, $J_4 = 13.5$ Hz), 1.68 (dddd, 1H, $J_1 = 1.5$, $J_2 = 3.5$, $J_3 = 6.5$, $J_4 = 13.5$ Hz), 2.09 (q, 2H, $J = 7.5$ Hz), 2.05-2.13 (m, 1H), 2.54 (ddd, 1H, $J_1 = J_2 = 6.0$, $J_3 = 13.0$ Hz), 2.82 (ddd, 1H, $J_1 = 6.5$, $J_2 = 11.5$, $J_3 = 18.0$ Hz), 2.93 (ddd, 1H, $J_1 = J_2 = 5.5$, $J_3 = 13.0$ Hz), 3.00 (ddd, 1H, $J_1 = 1.5$, $J_2 = 6.0$, $J_3 = 18.0$ Hz), 4.25 (d, 1H, $J = 5.0$ Hz), 6.85 (d, 1H, $J = 7.5$ Hz), 6.96-6.98 (m, 2H), 7.03 (dd, 1H, $J_1 = J_2 = 7.0$ Hz), 7.12 (dddd, 1H, $J_1 = J_2 = 1.5$ and $J_3 = J_4 = 7.5$ Hz), 7.15-7.26 (m, 4H), 7.72 (brt, 1H). ^{13}C NMR (100 MHz, CDCl_3): δ 173.8 (CO), 143.1, 138.8, 136.4, 130.6, 130.0, 128.9, 128.1, 126.5, 126.2, 125.9, 47.9 (C1), 42.8 (C11), 38.8 (C2), 29.7 ($\underline{\text{CH}_2\text{CH}_3}$), 28.8 (C4), 21.6 (C3), 9.9 ($\text{CH}_2\underline{\text{CH}_3}$). ESI MS (m/z): 294 ($\text{M}+1$) $^+$. HRMS (ESI): m/z calculated for $\text{C}_{20}\text{H}_{23}\text{NO}$, $[\text{M} + \text{H}]^+$ 294.1858. Found: 294.1858.

(\pm)-*N*-[(4-Phenyl-1,2,3,4-tetrahydroquinolin-3-yl)methyl]propionamide (12). A solution of 4-phenylquinoline-3-carbonitrile¹⁸ (0.230 g, 1 mmol) in THF (5 mL) and 2M NH_3 in EtOH (0.6 mL) was hydrogenated (4 atm) over Raney-Ni for 16 h at 60 °C. The catalyst was filtered on Celite, the filtrate was concentrated *in vacuo*, and the residue partitioned between EtOAc and water. The organic phase was washed with brine, dried (Na_2SO_4) and evaporated under reduced pressure to give the corresponding crude oily amine which was used without any further purification. Et_3N (0.14 mL, 1 mmol) and propionic anhydride (0.13 mL, 1 mmol) were added to a cold solution of the above crude amine in THF (6 mL) and the resulting mixture was stirred at room temperature for 1 h. The solvent was removed by distillation under reduced pressure, the residue was taken up in EtOAc and washed with a saturated aqueous solution of NaHCO_3 and then with brine. After drying over Na_2SO_4 , the solvent was removed by distillation *in vacuo* to give a crude product that was purified by silica gel flash chromatography (EtOAc-MeOH 98:2 as eluent) and crystallization. White solid, (CHCl_3 -hexane); 46% yield. ^1H NMR (400 MHz, acetone- d_6): δ 1.05 (t, 3H, $J = 7.5$ Hz), 2.15 (q, 2H, $J = 7.5$

Hz), 2.28-2.36 (m, 1H), 2.71 (ddd, 1H, $J_1 = 6.0$, $J_2 = 9.0$, $J_3 = 14.0$ Hz), 3.05 (ddd, 1H, $J_1 = 3.0$, $J_2 = J_3 = 11.5$ Hz), 3.16 (ddd, 1H, $J_1 = J_2 = 5.5$, $J_3 = 14.0$ Hz), 3.29 (dddd, 1H, $J_1 = 1.0$, $J_2 = J_3 = 4.0$, $J_4 = 11.5$ Hz), 4.16 (d, 1H, $J = 4.5$), 5.27 (brs, 1H), 6.63 (dd, 1H, $J_1 = 1.0$, $J_2 = 8.0$ Hz), 6.78 (dd, 1H, $J_1 = 1.0$, $J_2 = 7.5$ Hz), 6.93 (ddd, 1H, $J_1 = 1.5$, $J_2 = J_3 = 8.0$ Hz), 7.00 (brs, 1H), 7.14-7.21 (m, 3H), 7.25-7.29 (m, 2H). ESI MS (m/z): 295 (M+H)⁺.

(±)-cis-N-[(1-Methyl-4-phenyl-1,2,3,4-tetrahydroquinolin-3-yl)methyl]propionamide (13).

Sodium cyanoborohydride (0.1 g, 1.20 mmol) and a 37% aqueous solution of HCHO (0.5 mL) were added to a solution of **12** (0.5 mmol), in MeOH (5 mL) and AcOH (to pH = 5). The resulting mixture was stirred at room temperature for 1 h and then at 40 °C for 3 h. A 30% NaOH aqueous solution was added, and the aqueous phase was extracted with EtOAc. After drying over Na₂SO₄, the combined organic layers were concentrated by distillation under reduced pressure to give a crude residue which was purified by silica gel flash chromatography (cyclohexane-EtOAc 6:4 as eluent) and crystallization. White solid, mp 167-8 °C (EtOAc-petroleum ether); 72% yield. ¹H NMR (400 MHz, DMSO-*d*₆): δ 0.99 (t, 3H, $J = 8.0$ Hz), 2.09 (q, 2H, $J = 8.0$ Hz), 2.28 (dddd, 1H, $J_1 = 4.0$, $J_2 = 4.5$, $J_3 = 5.0$, $J_4 = 9.0$, $J_5 = 11.5$ Hz), 2.52 (dd, 1H, $J_1 = 9.0$ Hz, $J_2 =$ not computable), 2.93 (dd, 1H, $J_1 = J_2 = 11.5$ Hz), 2.95 (s, 3H), 2.96 (dd, 1H, $J_1 = 5$ Hz, $J_2 =$ n.c.), 3.10 (ddd, 1H, $J_1 = 1$, $J_2 = 4.0$, $J_3 = 11.5$ Hz), 4.13 (dd, 1H, $J_1 = 1.0$, $J_2 = 4.5$ Hz), 6.47 (ddd, 1H, $J_1 = 1.0$, $J_2 = J_3 = 7.5$ Hz), 6.70 (d, 1H, $J_1 = 8.0$ Hz), 6.78 (dd, 1H, $J_1 = 1.5$, $J_2 = 7.5$ Hz), 6.98-7.00 (m, 2H), 7.05 (ddd, 1H, $J_1 = 1.5$, $J_2 = 7.5$, $J_3 = 8.0$ Hz), 7.16-7.19 (m, 1H), 7.23-7.27 (m, 2H), 7.76 (brt, 1H). ¹³C NMR (100 MHz, MeOD): δ 175.7 (CO), 145.9 (C9), 142.5 (C10), 129.54 (C5), 129.47, 127.5, 127.4 (C7), 126.0, 124.5, 116.0 (C6), 110.6 (C8), 49.4 (C11), 46.2 (C4), 40.5 (C2), 37.8 (NCH₃), 36.7 (C3), 28.7 (CH₂CH₃), 9.1 (CH₂CH₃). ESI MS (m/z): 309 (M+H)⁺. HRMS (ESI): m/z calculated for C₂₀H₂₄N₂O, [M + H]⁺ 309.1967. Found: 309.1967.

(±)-*N*-[(1,2,3,4-Tetrahydroquinolin-3-yl)methyl]acetamide (**14**). To prepare this compound, quinoline-3-carbonitrile (0.154 g, 1 mmol) was submitted to catalytic hydrogenation (Raney-Ni, H₂ 4 atm, 60 °C, 16 h) and the corresponding methanamine was *N*-acylated with acetic anhydride following the procedure described for the synthesis of **12**. Purification by silica gel flash chromatography (EtOAc-MeOH 95:5 as eluent) and crystallization. White solid, mp 126-7 °C (diethyl ether-petroleum ether), 70% yield. ¹H NMR (200 MHz, CDCl₃): δ 1.98 (s, 3H), 2.18-2.23 (m, 1H), 2.53 (dd, 1H, *J*₁ = 8.0, *J*₂ = 16.0 Hz), 2.86 (dd, 1H, *J*₁ = 5.0, *J*₂ = 11.0 Hz) 3.05 (dd, 1H, *J*₁ = 8.0, *J*₂ = 11.0 Hz), 3.17-3.43 (m, 3H), 3.83 (brs, 1H), 5.68 (brs, 1H), 6.49 (d, 1H, *J* = 7.5 Hz), 6.63 (dd, 1H, *J*₁ = 1.0, *J*₂ = 7.5 Hz), 6.94-7.02 (m, 2H). ¹³C NMR (100 MHz, CDCl₃): δ 170.4, 144.0, 129.7, 126.9, 120.0, 117.6, 114.3, 44.7, 42.3, 32.5, 30.7, 23.3. EI MS (*m/z*): 204 (M⁺), 130 (100). HRMS (ESI): *m/z* calculated for C₁₂H₁₆N₂O, [M + H]⁺ 205.1341. Found: 205.1341.

***N*¹-Alkylation of *N*-[(1,2,3,4-tetrahydroquinolin-3-yl)methyl]acetamide: general procedure (**15a-d**).** A solution of *N*-[(1,2,3,4-tetrahydroquinolin-3-yl)methyl]acetamide **14** (0.204 g, 1 mmol), Et₃N (0.8 mL, 5.7 mmol) and the suitable alkyl halide (5 mmol) in dry toluene (6 mL) was heated for 1-24 h. After cooling to room temperature, the reaction mixture was poured into water, extracted with EtOAc (4x), and the combined organic phases were washed with brine and dried (Na₂SO₄). The solvent was removed by distillation *in vacuo* and the residue was purified by silica gel flash chromatography and/or crystallization.

(±)-*N*-[(1-Methyl-1,2,3,4-tetrahydroquinolin-3-yl)methyl]acetamide (**15a**). Methyl iodide as alkylating reagent; 70 °C in a sealed vessel for 16 h. Purification by silica gel flash chromatography (EtOAc-cyclohexane 8:2 as eluent) and crystallization. Beige solid, mp 109-10 °C (diethyl ether-petroleum ether), 68% yield. ¹H NMR (200 MHz, CDCl₃): δ 1.99 (s, 3H), 2.18-2.34 (m, 1H), 2.54

(dd, 1H, $J_1 = 8.5$, $J_2 = 16.0$ Hz), 2.85 (dd, 1H, $J_1 = 5.0$, $J_2 = 11.0$ Hz) 2.88 (s, 3H), 2.98 (dd, 1H, $J_1 = 8.0$, $J_2 = 11.0$ Hz), 3.16-3.49 (m, 3H), 5.63 (brs, 1H), 6.58-6.66 (m, 2H), 6.96 (d, 1H, $J = 7.5$ Hz), 7.09 (dd, 1H, $J_1 = 1.0$, $J_2 = 7.5$ Hz). ^{13}C NMR (100 MHz, CDCl_3): δ 170.3, 145.7, 129.2, 127.3, 121.6, 117.3, 111.6, 54.3, 42.5, 39.5, 32.7, 31.4, 23.3. ESI MS (m/z): 219 ($\text{M}+\text{H}$)⁺. HRMS (ESI): m/z calculated for $\text{C}_{13}\text{H}_{18}\text{N}_2\text{O}$, $[\text{M} + \text{H}]^+$ 219.1497. Found: 219.1497.

(±)-*N*-[(1-Ethyl-1,2,3,4-tetrahydroquinolin-3-yl)methyl]acetamide (15b). Ethyl iodide as alkylating reagent; 100 °C in a sealed vessel for 16 h. Purification by silica gel flash chromatography (EtOAc-cyclohexane 8:2 as eluent) and crystallization. Beige solid, mp 84-5 °C (diethyl ether-petroleum ether), 81% yield. ^1H NMR (200 MHz, CDCl_3): δ 1.12 (t, 3H, $J = 7.0$ Hz), 1.99 (s, 3H), 2.13-2.32 (m, 1H), 2.52 (dd, 1H, $J_1 = 8.5$, $J_2 = 16.0$ Hz), 2.83 (dd, 1H, $J_1 = 5.0$, $J_2 = 16.0$ Hz), 3.02 (dd, 1H, $J_1 = 8.0$, $J_2 = 11.0$ Hz), 3.13-3.49 (m, 5H), 5.65 (brs, 1H), 6.53-6.62 (m, 2H), 6.96 (d, 1H, $J = 7.5$ Hz), 7.06 (dd, 1H, $J_1 = 1.5$, $J_2 = 7.5$ Hz). ^{13}C NMR (100 MHz, CDCl_3): δ 170.4, 144.3, 129.6, 127.3, 120.9, 116.1, 110.8, 51.3, 45.5, 42.5, 32.5, 31.8, 23.3, 10.6. EI MS (m/z): 232 (M^+), 130 (100). HRMS (ESI): m/z calculated for $\text{C}_{14}\text{H}_{20}\text{N}_2\text{O}$, $[\text{M} + \text{H}]^+$ 233.1654. Found: 233.1654.

(±)-*N*-[(1-Benzyl-1,2,3,4-tetrahydroquinolin-3-yl)methyl]acetamide (15c): Benzyl bromide as alkylating reagent; 1 h under reflux. Purification by silica gel flash chromatography (EtOAc as eluent) and crystallization. White solid, mp 97-8 °C (diethyl ether-petroleum ether); 85% yield. ^1H NMR (200 MHz, CDCl_3): δ 1.91 (s, 3H), 2.21-2.34 (m, 1H), 2.57 (dd, 1H, $J_1 = 8.5$, $J_2 = 16.0$ Hz), 2.92 (dd, 1H, $J_1 = 5.0$, $J_2 = 15.0$ Hz) 3.12 (ddd, 1H, $J_1 = 1.0$, $J_2 = 7.5$, $J_3 = 11.0$ Hz), 3.22-3.30 (m, 2H), 3.34 (ddd, 1H, $J_1 = 1.5$, $J_2 = 3.5$, $J_3 = 11.5$ Hz), 4.36 (d, 1H, $J = 16.5$ Hz), 4.56 (d, 1H, $J = 16.5$ Hz), 5.41 (brs, 1H), 6.54-6.65 (m, 2H), 6.97-7.05 (m, 2H), 7.22-7.37 (m, 5H). ^{13}C NMR (100 MHz, CDCl_3): δ 170.3, 145.1, 138.7, 129.6, 128.7, 127.4, 127.1, 126.9, 120.5, 116.6, 111.2, 55.1, 51.9, 42.1, 32.4,

31.7, 23.3. EI MS (m/z): 294 (M^+), 144 (100). HRMS (ESI): m/z calculated for $C_{19}H_{22}N_2O$, $[M + H]^+$ 295.1810. Found: 295.1810.

(±)-*N*-[(1-Phenylethyl-1,2,3,4-tetrahydroquinolin-3-yl)methyl]acetamide (15d). 2-Phenylethyl bromide as alkylating reagent; 16 h under reflux. Purification by silica gel flash chromatography (EtOAc as eluent) and crystallization. White solid, mp 123-4 °C (CH_2Cl_2 -petroleum ether); 46% yield. 1H NMR (200 MHz, $CDCl_3$): δ 1.92 (s, 3H), 2.02-2.20 (m, 1H), 2.49 (dd, 1H, $J_1 = 8.0$, $J_2 = 16.0$ Hz), 2.77-2.96 (m, 4H), 3.08-3.18 (m, 3H), 3.46-3.56 (m, 2H), 5.22 (brs, 1H), 6.57-6.70 (m, 2H), 6.97 (dd, 1H, $J_1 = 1.0$, $J_2 = 7.5$ Hz), 7.07-7.15 (m, 1H), 7.19-7.37 (m, 5H). ^{13}C NMR (100 MHz, $CDCl_3$): δ 170.2, 144.5, 140.0, 129.6, 129.0, 128.5, 127.3, 126.2, 120.6, 116.1, 110.4, 53.3, 52.6, 42.2, 32.8, 32.3, 31.7, 23.3. ESI MS (m/z): 309 ($M+H$) $^+$. HRMS (ESI): m/z calculated for $C_{20}H_{24}N_2O$, $[M + H]^+$ 309.1967. Found: 309.2012.

(±)-*N*-[(1-Phenyl-1,2,3,4-tetrahydroquinolin-3-yl)methyl]acetamide (15e). This product was prepared by N^1 -arylation of **14** with bromobenzene following the procedure described for the synthesis of **7a**. White solid, mp 144-5 °C (diethyl ether-petroleum ether); 29% yield. 1H NMR (400 MHz, $DMSO-d_6$): δ 1.81 (s, 3H), 2.13 (dddddd, 1H, $J_1 = 3.5$, $J_2 = 4.5$, $J_3 = J_4 = 6.0$, $J_5 = 9.0$, $J_6 = 10.0$ Hz), 2.52 (dd, 1H, $J_1 = 10.0$, $J_2 = 16.0$ Hz), 2.84 (ddd, 1H, $J_1 = 1.5$, $J_2 = 4.5$, $J_3 = 16.0$ Hz), 3.06 (dd, 1H, $J_1 = 6.0$, $J_2 = 13.5$ Hz), 3.13 (dd, 1H, $J_1 = 6.0$, $J_2 = 13.5$ Hz), 3.25 (dd, 1H, $J_1 = 9.0$, $J_2 = 11.5$ Hz), 3.63 (ddd, 1H, $J_1 = 1.5$, $J_2 = 3.5$, $J_3 = 11.5$ Hz), 6.56 (dd, 1H, $J_1 = 1.0$, $J_2 = 8.0$ Hz), 6.65 (dddd, 1H, $J_1 = J_2 = 1.0$, $J_3 = J_4 = 7.5$ Hz), 6.88 (dddd, 1H, $J_1 = J_2 = 1.5$, $J_3 = J_4 = 8.0$ Hz), 7.01-7.40 (m, 6H), 7.95 (brt, 1H). ^{13}C NMR (100 MHz, $CDCl_3$): δ 170.3 (CO), 147.9 (C9), 143.8 (C10), 129.8 (C5), 129.5, 126.5 (C7), 124.7, 124.0, 122.4, 118.6 (C6), 115.4 (C8), 53.5 (C4), 42.2 (C11), 33.1 (C3), 31.5

(C2), 23.3 (CH₃). EI MS (*m/z*): 280 (M⁺), 208 (100). HRMS (ESI): *m/z* calculated for C₁₈H₂₀N₂O, [M + H]⁺ 281.1654. Found: 281.1692.

Separation of (±)-15e by semi-preparative reverse-phase Chiral HPLC

The enantiomers of compound (±)-15e were completely resolved by a semi-preparative process using a RegisCell column (Ø=1 cm, l=25 cm, 5 µm), eluting with hexane/isopropyl alcohol 95/5 at room temperature with a flow rate of 4 mL min⁻¹ (Supplementary Figures S11-13). 11 batches of about 3 mg of (±)-15e were processed and the eluate was properly partitioned according to the UV profile, affording both (-)- and (+)-15e enantiomers. Analytical control of collected fractions was performed on a Daicel Chiralcel OD-H column (Ø=0.46 cm, l=15 cm, 5 µm) eluting with hexane/isopropyl alcohol 95/5 at room temperature at a flow rate of 0.5 mL min⁻¹ and UV detection at λ=285 nm. The combined fractions containing each enantiomer were concentrated by distillation at reduced pressure. The chiral stationary phase of both RegisCell and OD-H columns was tris-(3,5-dimethylphenyl) carbamoyl cellulose.

(+)-*N*-[(1-Phenyl-1,2,3,4-tetrahydroquinolin-3-yl)methyl]acetamide [(+)-15e]. Amorphous solid, 11.0 mg, *ee*: 99.9% determined by analytical chiral HPLC: t_R=18.12 min, [α]_D²⁰ = +24.5 ° (c: 0.5, CH₂Cl₂).

(-)-*N*-[(1-Phenyl-1,2,3,4-tetrahydroquinolin-3-yl)methyl]acetamide [(-)-15e] Amorphous solid, 11.5 mg, *ee*: 98.9% determined by analytical chiral HPLC: t_R=22.49 min, [α]_D²⁰ = -24.2 ° (c: 0.5, CH₂Cl₂).

Pharmacology

Reagents and Chemicals

2-[¹²⁵I]-Iodomelatonin (2200 Ci/mmol) was purchased from NEN (Boston, MA). Other drugs and chemicals were purchased from Sigma-Aldrich (Saint Quentin, France).

Cell Culture

CHO cell lines stably expressing the human melatonin MT₁ or MT₂ receptors were grown in DMEM medium supplemented with 10% fetal calf serum, 2 mM glutamine, 100 IU/mL penicillin and 100 µg/ml streptomycin. Grown at confluence at 37 °C (95% O₂/5% CO₂), they were harvested in PBS containing EDTA 2 mM and centrifuged at 1000 g for 5 min (4 °C). The resulting pellet was suspended in TRIS 5 mM (pH 7.5), containing EDTA 2 mM and homogenized using a Kinematica polytron. The homogenate was then centrifuged (95000 g, 30 min, 4 °C) and the resulting pellet suspended in 75 mM TRIS (pH 7.5), 12.5 mM MgCl₂ and 2 mM EDTA. Aliquots of membrane preparations were stored at -80 °C until use.

Binding Assays

2-[¹²⁵I]iodomelatonin binding assay conditions were essentially as previously described.²⁶ Briefly, binding was initiated by addition of membrane preparations from stable transfected CHO cells diluted in binding buffer (50 mM Tris-HCl buffer, pH 7.4 containing 5 mM MgCl₂) to 2-[¹²⁵I]-iodomelatonin (20 pM for MT₁ and MT₂ receptors) and the tested drug. Nonspecific binding was defined in the presence of 1 µM melatonin. After 120 min incubation at 37 °C, reaction was stopped by rapid filtration through GF/B filters presoaked in 0.5% (v/v) polyethylenimine. Filters were washed three times with 1 mL of ice-cold 50 mM Tris-HCl buffer, pH 7.4.

Data from the dose-response curves (7 concentrations in duplicate) were analyzed using the program PRISM (Graph Pad Software Inc., San Diego, CA) to yield IC₅₀ (inhibitory concentration 50). Results are expressed as $K_i = IC_{50} / 1 + ([L]/K_D)$, where [L] is the concentration of radioligand used in the

assay and K_D , the dissociation constant of the radioligand characterizing the membrane preparation.²⁷ K_i (nM) values are geometric mean values of at least two separate experiments performed in duplicate.

Functional Assays

[³⁵S]GTP γ S binding assay was performed according to published methodology.²⁶ Briefly, membranes from transfected CHO cells expressing MT₁ or MT₂ receptor subtype and compounds were diluted in binding buffer (20 mM HEPES, pH 7.4, 100 mM NaCl, 3 μ M GDP, 3 mM MgCl₂, and 20 μ g/mL saponin). Incubation was started by the addition of 0.2 nM [³⁵S]GTP γ S to membranes (20 μ g/mL) and drugs, and further followed for 1 h at room temperature. Nonspecific binding was defined using cold GTP γ S (10 μ M). Reaction was stopped by rapid filtration through GF/B filters followed by three successive washes with ice cold buffer.

Usual levels of [³⁵S]GTP γ S binding (expressed in dpm) were for CHO-MT₁ or MT₂ membranes: 2000 for basal activity, 8000 in the presence of melatonin 1 μ M, and 180 in the presence of GTP γ S 10 μ M which defined the nonspecific binding. Data from the dose-response curves (7 concentrations in duplicate) were analyzed by using the program PRISM (Graph Pad Software Inc., San Diego, CA) to yield EC₅₀ (Effective concentration 50 %) and E_{max} (maximal effect) for agonists. EC₅₀ (nM) values are geometric mean values of at least two separate experiments performed in duplicate.

Molecular modelling

Compound structures were built using Maestro 11.0²⁸ and minimized with Macromodel 11.4²⁹ by applying the OPLS3 force field³⁰ and the GB/SA continuum solvation model for water to an energy gradient of 0.05 kJ mol⁻¹Å⁻¹. Well-tempered metadynamics simulations of compounds (1*S*,2*S*)-**10** and (1*S*,2*R*)-**11** were performed using Desmond 4.8³¹ implemented within the Schrodinger 2016-4 suite, by applying the OPLS3 force field. The minimized structures of compound (1*S*,2*S*)-**10** and (1*S*,2*R*)-

11 were solvated with explicit TIP3P water, placing the simulation box boundaries 10 Å far from the ligand atoms on each side. The systems were equilibrated using the default relaxation protocol implemented in Desmond 4.8. (1*S*,2*S*)-**10** and (1*S*,2*R*)-**11** were then submitted to a 50 ns-long well-tempered metadynamics simulation using the Langevin coupling scheme in the NVT ensemble, and setting the temperature at 298 K. Dihedral angles τ_1 and τ_2 (Figure 3a) were chosen as collective variables. The initial height and width of the Gaussian potentials were set to 0.03 kcal mol⁻¹ and 2 °, respectively, while the deposition rate was set to 0.09 ps. In well-tempered metadynamics, the potential heights w_j are resized taking into account the value of the accumulated bias potential $V_{(s,t)}$:

$$w_j = w \times \exp\left(\frac{V_{(s,t_j)}}{k_B \Delta T}\right)$$

where k_B is the Boltzmann constant, while the sampling temperature ΔT was set to 600 K. The convergence was assessed by evaluating the evolution of the free-energy profiles and of the relative free-energy levels of the global and local minima throughout the simulation time. Free-energy surfaces were calculated every 2.5 ns, and the simulations were considered as converged when free-energy differences among the global and local minima became constant, after 25 ns of simulation (see Supporting Information Figures S7 and S8). The FES obtained after 25 ns are represented in Figure 3b and Figure 3c for (1*S*,2*S*)-**10** and (1*S*,2*R*)-**11**, respectively. The well-tempered metadynamics simulations were replicated for three times for each compound, changing the seed to assign the initial velocities. At convergence, the free-energy surfaces obtained from each simulation performed for compounds (1*S*,2*S*)-**10** and (1*S*,2*R*)-**11** were superimposable. The conformational equilibria resulting from these metadynamics simulations in water were compared with the results of NMR experiments performed in DMSO. We had already demonstrated that the free energy surfaces obtained from metadynamics simulations in different solvents are comparable, in terms of location of minima and energy difference.¹⁴

In order to assess the metadynamics accuracy, a plain molecular dynamics (MD) simulation of compound (1*S*,2*R*)-**11** was also performed. The MD simulation was performed in the NVT ensemble, using the Langevin coupling scheme and setting the temperature at 298 K. The simulation was carried out for 1 μ s, collecting one frame every 100 ps. The frames were then projected onto a τ_1 - τ_2 grid, and the free-energy for each cell *i* of the grid was calculated from the probability distribution of states as:

$$\Delta G_i = -RT \times \ln N_i/N_0$$

where N_i is the number of frames in the cell *i* and N_0 is the number of frames in the most populated cell. The FES thus obtained is represented in Supplementary Figure S9 and shows qualitative agreement with the result of metadynamics simulations.

Supporting information

The Supporting Information is available free of charge on the ACS Publications website. ¹H NMR spectra of compounds **10**, **11**, *cis*-**13** and **15e**, NOESY spectra of compounds *cis*-**13** and **15e**, free-energy surfaces obtained from plain molecular dynamics and metadynamics simulations of compounds (1*S*,2*S*)-**10** and (1*S*,2*R*)-**11**, HRMS spectra and purity of target compounds (PDF), analytical and semi-preparative HPLC chromatograms of racemic **15e** and its optically pure enantiomers.

Author Information

Corresponding Author

*Phone: +39 0722 303322. Fax: + 39 0722 303313. E-mail: gilberto.spadoni@uniurb.it.

Acknowledgment

The Authors thank Dr. Marta Rui for support of chiral resolution.

Notes

The authors declare no competing financial interest.

Abbreviations

BINAP, 2,2'-bis(diphenylphosphino)-1,1'-binaphthyl; DMEM, Dulbecco's Modified Eagle Medium; E_{max} , maximum activation of receptor; GTP γ S, guanosine 5'-O-(3-thiotriphosphate); HPLC, high-performance liquid chromatography; MD, molecular dynamics; MLT, melatonin; MT₁, melatonin receptor subtype 1; MT₂, melatonin receptor subtype 2; NOE, nuclear Overhauser effect; NOESY, nuclear Overhauser effect spectroscopy; PBS, phosphate-buffered saline; THF, tetrahydrofuran.

References

- ¹ Hardeland, R.; Cardinali, D. P.; Srinivasan, V.; Spence, D. W.; Brown, G.M.; Pandi-Perumal, S.R. Melatonin--a pleiotropic, orchestrating regulator molecule. *Prog. Neurobiol.* **2011**, *93*, 350–384.
- ² Liu, J.; Clough, S. J.; Hutchinson, A. J.; Adamah-Biassi, E. B.; Popovska-Gorevski, M.; Dubocovich, M. L. MT₁ and MT₂ melatonin receptors: a therapeutic perspective. *Annu. Rev. Pharmacol. Toxicol.* **2016**, *56*, 361–383.
- ³ Gatti, G.; Lucini, V.; Dugnani, S.; Calastretti, A.; Spadoni, G.; Bedini, A.; Rivara, S.; Mor, M.; Canti, G.; Scaglione, F.; Bevilacqua, A. *Oncotarget.* **2017**, *8*, 68338-68353.

-
- ⁴ Jockers, R.; Delagrangue, P.; Dubocovich, M.L.; Markus R. P.; Renault N.; Tosini, G.; Cecon E.; Zlotos, D. P. Update on melatonin receptors: IUPHAR Review 20. *Br. J. Pharmacol.* **2016**, *173*, 2702–2725.
- ⁵ Baba, K.; Benleulmi-Chaachoua, A.; Journé, A. S.; Kamal, M.; Guillaume, J. L.; Dussaud, S.; Gbahou, F.; Yettou, K.; Liu, C.; Contreras-Alcantara, S.; Jockers, R.; Tosini, G. Heteromeric MT₁/MT₂ melatonin receptors modulate photoreceptor function. *Sci Signal.* **2013**, *6*, ra89.
- ⁶ Kamal, M.; Gbahou, F.; Guillaume, J. L.; Daulat, A. M.; Benleulmi-Chaachoua, A.; Luka, M.; Chen, P.; Kalbasi Anaraki, D.; Baroncini, M.; Mannoury la Cour, C.; Millan, M.J.; Prevot, V.; Delagrangue, P.; Jockers, R. Convergence of melatonin and serotonin (5-HT) signaling at MT₂/5-HT_{2C} receptor heteromers. *J. Biol. Chem.* **2015**, *290*, 11537–11546.
- ⁷ Carocci, A.; Catalano, A.; Sinicropi, M. S. Melatonergic drugs in development. *Clin. Pharmacol.* **2014**, *6*, 127–137.
- ⁸ Zlotos, D. P.; Jockers, R.; Cecon, E.; Rivara, S.; Witt-Enderby, P. A. MT₁ and MT₂ melatonin receptors: ligands, models, oligomers, and therapeutic potential. *J. Med. Chem.* **2014**, *57*, 3161–3185.
- ⁹ Rivara, S.; Lodola, A.; Mor, M.; Bedini, A.; Spadoni, G.; Lucini, V.; Pannacci, M.; Fraschini, F.; Scaglione, F.; Sanchez, R. O.; Gobbi, G.; Tarzia, G. N-(Substituted-anilinoethyl)amides: design, synthesis, and pharmacological characterization of a new class of melatonin receptor ligands. *J. Med. Chem.* **2007**, *50*, 6618–6626.
- ¹⁰ Rivara, S.; Vacondio, F.; Fioni, A.; Silva, C.; Carmi, C.; Mor, M.; Lucini, V.; Pannacci, M.; Caronno, A.; Scaglione, F.; Gobbi, G.; Spadoni, G.; Bedini, A.; Orlando, P.; Lucarini, S.; Tarzia, G. N-(Anilinoethyl)amides: design and synthesis of metabolically stable, selective melatonin receptor ligands. *ChemMedChem* **2009**, *4*, 1746–1755.
- ¹¹ Lopez-Canul, M.; Palazzo, E.; Dominguez-Lopez, S.; Luongo, L.; Lacoste, B.; Comai, S.; Angeloni, D.; Fraschini, F.; Boccella, S.; Spadoni, G.; Bedini, A.; Tarzia, G.; Maione, S.; Granados-

Soto, V.; Gobbi, G. Selective melatonin MT2 receptor ligands relieve neuropathic pain through modulation of brainstem descending antinociceptive pathways. *Pain* **2015**, *156*, 305–317.

¹² Ochoa-Sanchez, R.; Comai, S.; Lacoste, B.; Bambico, F. R.; Dominguez-Lopez, S.; Spadoni, G.; Rivara, S.; Bedini, A.; Angeloni, D.; Fraschini, F.; Mor, M.; Tarzia, G.; Descarries, L.; Gobbi, G. Promotion of non-rapid eye movement sleep and activation of reticular thalamic neurons by a novel MT2 melatonin receptor ligand. *J. Neurosci.* **2011**, *31*, 18439–18452.

¹³ Ochoa-Sanchez, R.; Rainer, Q.; Comai, S.; Spadoni, G.; Bedini, A.; Rivara, S.; Fraschini, F.; Mor, M.; Tarzia, G.; Gobbi, G. Anxiolytic effects of the melatonin MT(2) receptor partial agonist UCM765: comparison with melatonin and diazepam. *Prog. Neuropsychopharmacol. Biol. Psychiatry* **2012**, *39*, 318–325.

¹⁴ Spadoni, G.; Bedini, A.; Lucarini, S.; Mari, M.; Caignard, D.-H.; Boutin, J. A.; Delagrangue, P.; Lucini, V.; Scaglione, F.; Lodola, A.; Zanardi, F.; Pala, D.; Mor, M.; Rivara, S. Highly potent and selective MT2 melatonin receptor full agonists from conformational analysis of 1-benzyl-2-acylaminomethyl-tetrahydroquinolines. *J. Med. Chem.* **2015**, *58*, 7512–7525.

¹⁵ Hardeland, R. Melatonin and synthetic melatonergic agonists in psychiatric and age-associated disorders: successful and unsuccessful approaches. *Curr. Pharm. Des.* **2016**, *22*, 1086–1101.

¹⁶ Wikstrom, H. V.; Carlsson, P. A. E.; Andersson, B. R.; Bengt, R.; Svensson, K. A. I.; Elebring, S. T.; Stjernlof, N. P.; Romero, A. G.; Haadsma, S. R.; Lin, C. H.; Ennis, M. D. Preparation of Centrally Acting 6,7,8,9-Tetrahydro-3H-benz[a]indole Heterocyclics. PCT Int. Appl. WO9111435 A1, 1991.

¹⁷ Xie, J. H.; Liu, S.; Huo, X. H.; Cheng, X.; Duan, H. F.; Fan, B. M.; Wang, L. X.; Zhou, Q. L. Ru(II)-SDP-complex-catalyzed asymmetric hydrogenation of ketones. Effect of the alkali metal cation in the reaction. *J. Org. Chem.* **2005**, *70*, 2967–2973.

¹⁸ Guo, P.; Joo, J. M.; Rakshit, S.; Sames, D. C.-H. Arylation of pyridines: high regioselectivity as a consequence of the electronic character of C-H bonds and heteroarene ring. *J. Am. Chem. Soc.* **2011**, *133*, 16338–16341.

-
- ¹⁹ Dubocovich, M. L.; Masana, M. I.; Iacob, S.; Sauri, D. M. Melatonin receptor antagonists that differentiate between the human Mel1a and Mel1b recombinant subtypes are used to assess the pharmacological profile of the rabbit retina ML1 presynaptic heteroreceptor. *Naunyn-Schmiedeberg's Arch. Pharmacol.* **1997**, *355*, 365–375.
- ²⁰ Bedini, A.; Lucarini, S.; Spadoni, G.; Tarzia, G.; Scaglione, F.; Dugnani, S.; Pannacci, M.; Lucini, V.; Carmi, C.; Pala, D.; Rivara, S.; Mor, M. Toward the definition of stereochemical requirements for MT2-selective antagonists and partial agonists by studying 4-phenyl-2-propionamidotetralin derivatives. *J. Med. Chem.* **2011**, *54*, 8362–8372.
- ²¹ Rivara, S.; Mor, M.; Silva, C.; Zuliani, V.; Vacondio, F.; Spadoni, G.; Bedini, A.; Tarzia, G.; Lucini, V.; Pannacci, M.; Fraschini, F.; Plazzi, P. V. Three-dimensional quantitative structure-activity relationship studies on selected MT1 and MT2 melatonin receptor ligands: requirements for subtype selectivity and intrinsic activity modulation. *J. Med. Chem.* **2003**, *46*, 1429–1439.
- ²² Landagaray, E.; Ettaoussi, M.; Leclerc, V.; Traoré, B.; Perez, V.; Nosjean, O.; Boutin, J. A.; Caignard, D.-H.; Delagrange, P.; Berthelot, P.; Yous, S. New melatonin (MT1/MT2) ligands: design and synthesis of (8,9-dihydro-7H-furo[3,2-f]chromen-1-yl) derivatives. *Bioorg. Med. Chem.* **2014**, *22*, 986–996.
- ²³ Rivara, S.; Diamantini, G.; Di Giacomo, B.; Lamba, D.; Gatti, G.; Lucini, V.; Pannacci, M.; Mor, M.; Spadoni, G.; Tarzia, G. Reassessing the melatonin pharmacophore--enantiomeric resolution, pharmacological activity, structure analysis, and molecular modeling of a constrained chiral melatonin analogue. *Bioorg. Med. Chem.* **2006**, *14*, 3383–3391.
- ²⁴ Rossi, D.; Tarantino, M.; Rossino, G.; Rui, M.; Juza, M.; Collina, S. Approaches for multi-gram scale isolation of enantiomers for drug discovery. *Exp. Opin Drug Discov.* **2017**, *12*, 1253-1269.
- ²⁵ Rossi, D.; Marra, A.; Rui, M.; Brambilla, S.; Juza, M.; Collina, S. "Fit-for-purpose" development of analytical and (semi)preparative enantioselective high performance liquid and supercritical fluid

chromatography for the access to a novel σ_1 receptor agonist. *J. Pharm. Biomed. Anal.* **2016**, *118*, 363-369.

²⁶ Audinot, V.; Mailliet, F.; Lahaye-Brasseur, C.; Bonnaud, A.; Le Gall, A.; Amossé, C.; Dromaint, S.; Rodriguez, M.; Nagel, N.; Galizzi J. P.; Malpoux, B.; Guillaumet, G.; Lesieur, D.; Lefoulon, F.; Renard, P.; Delagrangé, P.; Boutin, J. A. New selective ligands of human cloned melatonin MT1 and MT2 receptors. *Naunyn-Schmiedeberg's Arch. Pharmacol.* **2003**, *367*, 553–561.

²⁷ Cheng, Y.; Prusoff W. H. Relationship between the inhibition constant (K_I) and the concentration of inhibitor which causes 50 per cent inhibition (I_{50}) of an enzymatic reaction. *Biochem. Pharmacol.* **1973**, *22*, 3099–3108.

²⁸ Schrödinger Release 2016-4: Maestro, Schrödinger, LLC, New York, NY, 2016

²⁹ Schrödinger Release 2016-4: MacroModel, Schrödinger, LLC, New York, NY, 2016.

³⁰ Harder, E.; Damm, W.; Maple, J.; Wu, C.; Reboul, M.; Xiang, J. Y.; Wang, L.; Lupyan, D.; Dahlgren, M. K.; Knight, J. L.; Kaus, J. W.; Cerutti, D. S.; Krilov, G.; Jorgensen, W. L.; Abel, R.; Friesner, R. A. OPLS3: a force field providing broad coverage of drug-like small molecules and proteins. *J. Chem. Theory Comput.* **2016**, *12*, 281–296.

³¹ Schrödinger Release 2016-4: Desmond Molecular Dynamics System, D. E. Shaw Research, New York, NY, 2016. Maestro-Desmond Interoperability Tools, Schrödinger, New York, NY, 2016.

Table of Contents Graphic

